

References and Notes

1. J. E. Galan, A. Collmer, *Science* **284**, 1322 (1999).
2. C. Hueck, *Microbiol. Mol. Biol. Rev.* **62**, 379 (1998).
3. G. R. Cornelis, F. Van Gijsegem, *Annu. Rev. Microbiol.* **54**, 735 (2000).
4. D. W. Gabriel, *Phys. Mol. Plant Pathol.* **55**, 205 (1999).
5. D. S. Guttman, J. T. Greenberg, *Mol. Plant-Microbe Interact.* **14**, 145 (2001).
6. J. T. Greenberg, *Annu. Rev. Plant Physiol. Plant Mol. Biol.* **48**, 525 (1997).
7. A. Collmer, *Curr. Opin. Plant Biol.* **1**, 329 (1998).
8. S. A. Lloyd, M. Norman, R. Rosqvist, H. Wolf-Watz, *Mol. Microbiol.* **39**, 520 (2001).
9. M. P. Sory, A. Boland, I. Lambermont, G. R. Cornelis, *Proc. Natl. Acad. Sci. U.S.A.* **92**, 11998 (1995).
10. M. P. Sory, G. R. Cornelis, *Mol. Microbiol.* **14**, 583 (1994).
11. M. B. Mudgett, B. J. Staskawicz, *Mol. Microbiol.* **32**, 927 (1999).
12. M. J. Axtell, T. W. McNellis, M. B. Mudgett, C. S. Hsu, B. J. Staskawicz, *Mol. Plant-Microbe Interact.* **14**, 181 (2001).
13. M. B. Mudgett et al., *Proc. Natl. Acad. Sci. U.S.A.* **97**, 13324 (2000).
14. J. R. Alfano, A. Collmer, *J. Bacteriol.* **179**, 5655 (1997).
15. Web note 1. Web tables and figures, as well as details of experimental procedures are available on Science Online at www.sciencemag.org/cgi/content/full/295/5560/1722/DC1.
16. V. T. Lee, O. Schneewind, *Mol. Microbiol.* **31**, 1619 (1999).
17. J. T. Greenberg, A. Guo, D. F. Klessig, F. M. Ausubel, *Cell* **77**, 551 (1994).
18. J. Glazebrook, E. E. Rogers, F. M. Ausubel, *Annu. Rev. Genet.* **31**, 547 (1997).
19. ———, *Genetics* **143**, 973 (1996).
20. Isolates were grown overnight to saturation, pooled into groups of eight, diluted by 1/10 and 1/20, and infiltrated into *A. thaliana* ecotype Columbia (*RPS2⁺*). Each dilution was individually tested on half of each of two replicate leaves of a single plant. Positive and negative HR controls were performed on each day. Plants were scored for HR by at least two people. Pools that induced an HR were deconvoluted down to a single HR-inducing colony. Each positive isolate was retested at least four times to confirm its ability to induce the HR. The region of insertion was sequenced in those strains that were scored as positive by either inverse or anchor PCR (42, 43). The complete sequence of *hop* genes was obtained from a *PmaES4326* cosmid library kindly provided by F. M. Ausubel (Department of Genetics, Harvard Medical School, and Department of Molecular Biology, Massachusetts General Hospital, Boston, MA, USA). This library was screened by PCR and colony filter hybridization for *hop*-containing clones following standard protocols. Most cosmids were positive for only one *hop* gene each. One cosmid contained *hopPmaB* as well as *avrPphE_{Pma}*. Sequence upstream of *avrPphE_{Pma}* had homology with *hrpK*, indicating that this cosmid is derived from the EEL (44). One cosmid contained *hrpW_{Pma}*, *avrE_{Pma}*, and *hopPtoA1_{Pma}*. Two cosmids contained *hopPmaD* as well as *hopPtoP_{Pma}*. DNA was extracted from positive cosmids and subcloned into pBS SK+ (Stratagene). Subclones were screened by PCR and PCR products spanning *hop* genes were sequenced and assembled using Lasergene (DNASTAR). Cosmid DNA was also digested with Eco RI and Hind III, run on a 0.8% agarose gel in 1× TBE, alkaline transferred to a positively charged nylon membrane, and probed with ³²P-radiolabeled cosmid DNA following standard protocols (45). Conservation of restriction fragments between clones hybridizing to the same cosmid DNA was used to identify overlapping cosmids. A cosmid containing *hopPmaC* overlapped by four hybridizing fragments with a cosmid containing *hopPmaL*.
21. Web note 2 (15).
22. J. Mansfield, C. Jenner, R. Hockenhull, M. A. Bennett, R. Stewart, *Mol. Plant-Microbe Interact.* **7**, 726 (1994).
23. C. Stevens et al., *Mol. Microbiol.* **29**, 165 (1998).
24. K. Orth et al., *Science* **290**, 1594 (2000).
25. J. M. Salmeron, B. J. Staskawicz, *Mol. Gen. Genet.* **239**, 6 (1993).
26. R. W. Jackson et al., *Proc. Natl. Acad. Sci. U.S.A.* **96**, 10875 (1999).
27. K. Makino et al., *Genes Genet. Syst.* **74**, 227 (1999).
28. K. Yokoyama et al., *Gene* **258**, 127 (2000).
29. T. Nambu, T. Minamino, R. M. Macnab, K. Kutsukake, *J. Bacteriol.* **181**, 1555 (1999).
30. C. H. Liao, D. E. McCallus, W. F. Fett, Y. G. Kang, *Can. J. Microbiol.* **43**, 425 (1997).
31. W. L. Kelley, *Trends Biochem. Sci.* **23**, 222 (1998).
32. Three full repeats of 37 or 38 amino acids (38 amino acids for the first repeat and 37 amino acids for the second and third) and a fourth partial repeat of 27 amino acids. The repeat sequence is RPPGAEQQAR-PETPPRSRPQTNsAPPPP-kAEPRPSG (46), starting at amino acid 194. Capital letters represent identities, small letters represent similar amino acids (based on PAM250), and a dash indicates a one amino acid insertion of a P in the first repeat. Repeat regions were identified with the aid of Dotlet (www.isrec.isb-sib.ch/java/dotlet/Dotlet.html) using a 15-amino acid window. Partially completed PtoDC3000 genome sequence obtained from TIGR (www.tigr.com).
33. K. Herbers, J. Conrads-Strauch, U. Bonas, *Nature* **356**, 172 (1992).
34. A. M. Barbieri, Q. Sha, P. Bette-Bobillo, P. D. Stahl, M. Vidal, *Infect. Immun.* **69**, 5329 (2001).
35. R. W. Innes, A. F. Bent, B. N. Kunkel, S. R. Bisgrove, B. J. Staskawicz, *J. Bacteriol.* **175**, 4859 (1993).
36. K. van Dijk et al., *J. Bacteriol.* **181**, 4790 (1999).
37. L. G. Rahme, M. N. Mindrinos, N. J. Panopoulos, *J. Bacteriol.* **174**, 3499 (1992).
38. O. Emanuelsson, H. Nielsen, S. Brunak, G. von Heijne, *J. Mol. Biol.* **300**, 1005 (2000).
39. B. Kenny, M. Jepsen, *Cell. Microbiol.* **2**, 579 (2000).
40. C. E. Stebbins, J. E. Galan, *Nature* **414**, 77 (2001).
41. D. Bowen et al., *Science* **280**, 2129 (1998).
42. H. Ochman, F. J. Ayala, D. L. Hartl, *Methods Enzymol.* **218**, 309 (1993).
43. D. S. Guttman, D. Charlesworth, *Nature* **393**, 263 (1998).
44. J. R. Alfano et al., *Proc. Natl. Acad. Sci. U.S.A.* **97**, 4856 (2000).
45. J. Sambrook, E. F. Fritsch, T. Maniatis, *Molecular Cloning, A Laboratory Manual* (Cold Spring Harbor Laboratory Press, Cold Spring Harbor, NY, ed. 2, 1989).
46. Single-letter abbreviations for the amino acid residues are as follows: A, Ala; C, Cys; D, Asp; E, Glu; F, Phe; G, Gly; H, His; I, Ile; K, Lys; L, Leu; M, Met; N, Asn; P, Pro; Q, Gln; R, Arg; S, Ser; T, Thr; V, Val; W, Trp; and Y, Tyr.
47. S. F. Altschul et al., *Nucleic Acids Res.* **25**, 3389 (1997).
48. Web note 3 (15).
49. S. Gaudriault, L. Malandrin, J. P. Paulin, M. A. Barby, *Mol. Microbiol.* **26**, 1057 (1997).
50. D.S.G. would like to acknowledge and thank A. Liu, J. Stavrindes, and L. Chu for their help with the screen. D.S.G. was supported by grants from NIH (NRSA GM020024) the Canadian National Science and Engineering Research Council (NSERC), the University of Toronto Connaught Fund, and the Canadian Foundation for Innovation. J.T.G. gratefully acknowledges funding by the Consortium for Biotechnology Research, Dow, Syngenta, the Pew Foundation, the University of Chicago Faculty Research Fund, and the University of Chicago's Division of Biological Sciences under the Research Resources Program for the Medical School of the Howard Hughes Medical Institute. Sequencing of *Pseudomonas syringae* pv *tomato* DC3000 was accomplished with support from the NSF. We thank A. Driks and L. Mets for helpful discussions.

7 November 2001; accepted 22 January 2002

Colorectal Cancer in Mice Genetically Deficient in the Mucin Muc2

Anna Velcich,^{1*} WanCai Yang,¹ Joerg Heyer,² Alessandra Fragale,¹ Courtney Nicholas,¹ Stephanie Viani,¹ Raju Kucherlapati,³ Martin Lipkin,⁴ Kan Yang,⁴ Leonard Augenlicht¹

The gastrointestinal tract is lined by a layer of mucus comprised of highly glycosylated proteins called mucins. To evaluate the importance of mucin in intestinal carcinogenesis, we constructed mice genetically deficient in Muc2, the most abundant secreted gastrointestinal mucin. Muc2^{-/-} mice displayed aberrant intestinal crypt morphology and altered cell maturation and migration. Most notably, the mice frequently developed adenomas in the small intestine that progressed to invasive adenocarcinoma, as well as rectal tumors. Thus, Muc2 is involved in the suppression of colorectal cancer.

Mucins are highly glycosylated proteins that are the major component of the mucus that lubricates and protects underlying intestinal epithe-

lium (1). Alterations of mucin expression and glycosylation have been observed in human colon cancer specimens (2), but the role of these proteins in tumorigenesis remains unclear. To evaluate the importance of mucin in the early stages of intestinal carcinogenesis, we generated mice genetically deficient in Muc2, the most abundant secreted gastrointestinal apomucin, which is the unglycosylated form of mucin (3, 4). Targeted inactivation of the *Muc2* gene was achieved by replacing a genomic fragment (5) harboring exons 2 to 4 of *Muc2* with a *phosphoglycerate kinase-neomycin* (PKG-Neo) cas-

¹Department of Oncology, Albert Einstein Cancer Center/Montefiore Medical Center, 111 East 210 Street, Bronx, NY 10467, USA. ²Memory Pharmaceuticals Corporation 100, Phillips Parkway, Montvale, NJ 07645, USA. ³Harvard Medical School, Brigham & Women's Hospital, 20 Shattuck Street, Boston, MA 02115, USA. ⁴Strang Cancer Prevention Center, 1300 York Avenue, New York, NY 10021, USA.

*To whom correspondence should be addressed. E-mail: velcich@aecom.yu.edu

sette (6). Six independent clones were identified by Southern blot analysis (6), displaying the appropriate recombinant event. *Muc2*^{+/-} F₁ progeny from two independently generated male chimeric mice were back-crossed to obtain F₂ mice of all three genotypes in the expected Mendelian ratio. These (C57BL/6J × 129/SvOla) F₂ to F₃ mice were used in the experiments described here. Heterozygous mice were indistinguishable from wild-type mice.

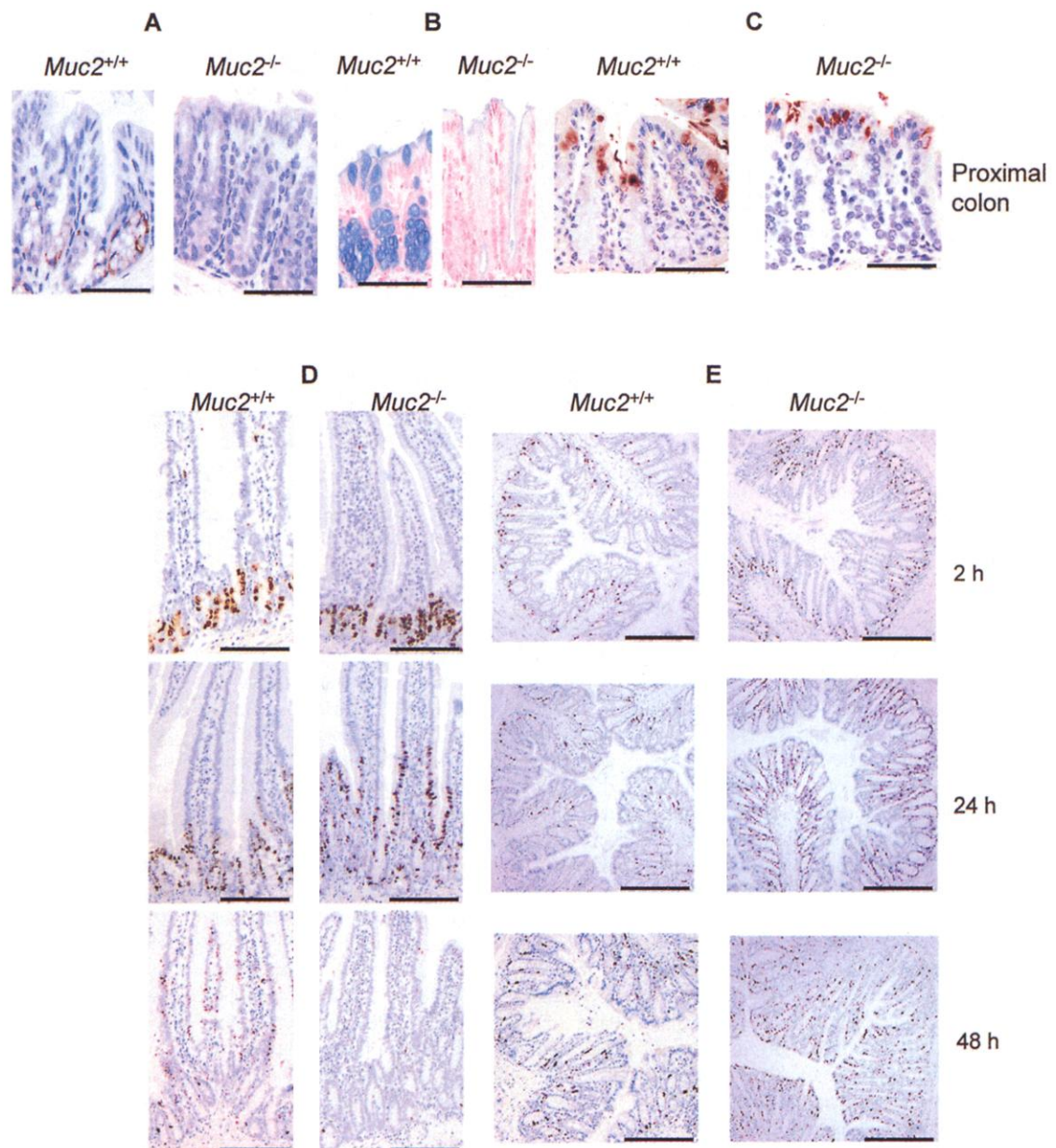
A probe specific for sequences downstream of the recombination event detected the characteristic polydisperse profile of *Muc2* messenger RNA (mRNA) in different portions of the intestine of *Muc2* wild-type mice (6). However, upon overexposure of the blot, the probe detected a similar band in the intestine of *Muc2*^{-/-} mice. Further

analysis demonstrated that this transcript was a hybrid *Muc2-Neo* mRNA, predicted to encode an 83 amino acid (aa) peptide containing the first 26 aa of the *Muc2* apoprotein (6). In agreement with the prediction, a polyclonal antibody (PH497) against deglycosylated gastrointestinal mucin stained goblet cells in the intestine of wild-type but not *Muc2*^{-/-} mice (Fig. 1A) (6). Thus, *Muc2*^{-/-} is a null mouse. Consistent with this, Alcian blue staining of acidic mucins in sections of the duodenum and the proximal and distal colon showed absence of recognizable goblet cells along the entire length of the intestine of *Muc2*^{-/-} mice (Fig. 1B) (6). The distal colon of *Muc2*^{-/-} mice showed residual light-blue staining toward the bottom of the crypt, but this pattern was distinct from that seen in wild-type mice.

The absence of goblet cells was not due to complete ablation of the differentiation pathway of this lineage because we could detect expression of intestinal trefoil factor (Itf), another product of fully differentiated goblet cells (7), by immunohistochemistry in cells that lacked the goblet cell morphology at a similar location in the intestine of both the homozygous mutant and the wild-type mice (Fig. 1C) (6). This suggests that at least some aspects of the differentiation program of the goblet cell lineage persist in *Muc2*^{-/-} mice. As assessed by RNA analysis and immunohistochemistry (6), there was no compensatory increase in expression of other apomucins (e.g., *Muc5ac*, *Muc3*, and *Muc13*) (8–10) in the intestine of *Muc2*^{-/-} mice.

Muc2^{-/-} mice gained weight at the same rate as their heterozygous and wild-type litter-

Fig. 1. Absence of *Muc2* apomucin and alteration of cell maturation in the *Muc2*^{-/-} intestine. Sections from proximal colon of wild-type and *Muc2*^{-/-} mice were stained in (A) with the polyclonal antibody PH497 that recognizes *Muc2*, in (B) with Alcian blue to identify goblet cells, and in (C) with a polyclonal antibody anti-Itf. (D and E) Immunohistochemical detection of BrdU-labeled cells in the intestine of wild-type and *Muc2*^{-/-} mice. Mice, injected with BrdU, were killed 2 hours after injection to determine the number of cells in S phase or 24 and 48 hours after BrdU injection to determine the rate of migration. Sections from the duodenum (D) or the distal colon (E) were stained with antibody to BrdU. Bars: (A) through (D), 25 μ m; (E), 100 μ m.



REPORTS

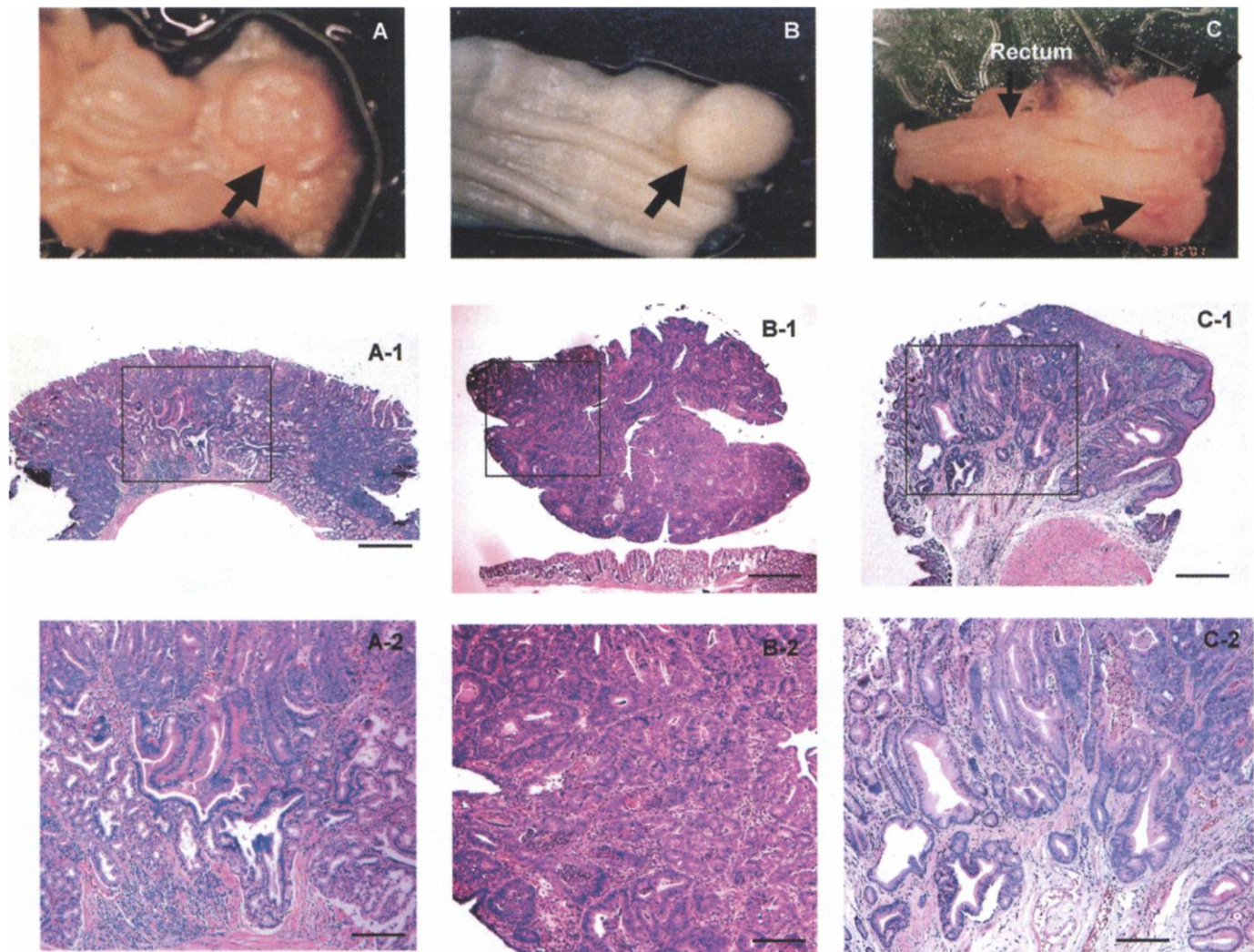


Fig. 2. Histopathology of tumors in *Muc2*^{-/-} mice. (A) Gross pathology of a tumor in the duodenum (black arrow); histopathological features of adenocarcinoma shown in (A-1) and (A-2). (B) Adenoma of the colon; histopathological features shown in (B-1) and (B-2). (C)

Adenocarcinoma of the rectum; histopathological features shown in (C-1) and (C-2). Small arrow, rectum; large arrow, tumor. Bars: (A-1) through (C-1), 250 μ m; (A-2) through (C-2), 100 μ m.

mates up to 12 months of age (11). However, random testing revealed occult fecal blood in some of the 6-month-old *Muc2*^{-/-} mice. Wild-type and *Muc2*^{-/-} mice were killed at 6 months and 1 year of age, and it was found that *Muc2*^{-/-} animals had developed gastrointestinal tumors. At the age of 1 year, 65% of the *Muc2*^{-/-} mice had tumors (Table 1) with a frequency of >1.5 tumors per mouse. In young mice, tumors were restricted to the small intestine, whereas in older mice tumors also appeared in the large intestine (Table 1), including the rectum. No tumors were detected in the stomach, where *Muc2* is not normally expressed.

Histopathological analysis revealed that the tumors were of epithelial origin and represented multiple stages of tumor progression. In mice younger than 6 months, tumors were classified as villous ($n = 2$), tubovillous ($n = 1$), and tubular adenomas ($n = 1$). In

older mice, the majority of the adenomas had progressed to invasive carcinomas (eight early and one advanced adenocarcinoma). In addition, 3 of 19 (15.7%) of *Muc2*^{-/-} mice developed rectal tumors. Figure 2 shows examples of the gross pathology and histopathology of the adenocarcinomas in duodenum and rectum and an adenoma in the colon.

To investigate the cellular mechanism by which inactivation of the *Muc2* gene caused tumor formation, we examined whether proliferation and rate of cell migration were altered in *Muc2*^{-/-} mice compared with wild-type littermates. Mice were injected with bromodeoxyuridine (BrdU) and killed 2, 24, or 48 hours later (6). At 2 hours after BrdU injection, *Muc2*^{-/-} mice exhibited a higher labeling index than wild-type mice in the duodenum [34.5%, (27.3 to 41.7, confidence intervals) in *Muc2*^{-/-} versus 24.9%, (9.9 to 39.9) in wild-type mice; $P < 0.068$], the proximal colon

[19.1%, (12.9 to 25.3), versus 10.9%, (2.8 to 19); $P < 0.05$], and the distal colon [15.6%, (6.0 to 25.2) versus 6.5%, (0.8 to 12.2); $P < 0.05$] (Fig. 1, D and E). The increased cell proliferation was accompanied by significant decreases in the percentage of apoptotic cells, measured by the TUNEL assay, in the duodenum [0.58%, (0.2 to 1) in *Muc2*^{-/-} versus 1.75%, (1 to 2.4) in wild-type mice], the proximal colon [0.43, (0.3 to 0.6) versus 1.22, (0.7 to 1.7)], and the distal colon [0.25, (0.1 to 0.4) versus 0.57, (0.4 to 0.8); in each case, $P < 0.01$]. Thus, the ratio of proliferating to apoptotic cells was highly elevated in the intestine of *Muc2*^{-/-} mice. Furthermore, both proximal and distal colon of *Muc2*^{-/-} mice displayed considerably elongated crypts as a result of an increased number of cells per crypt column (proximal colon, 18.2 ± 3.7 in *Muc2*^{-/-} versus 12.9 ± 3.1 in *Muc2*^{+/+}; distal colon, 29.7 ± 2.4 versus 20.8 ± 3.1 ; $P < 0.01$).

REPORTS

Table 1. Tumor incidence and frequency in the gastrointestinal tract of *Muc2* mice. Tumor incidence in wild-type and *Muc2*^{-/-} mice was compared using the Mantel-Haenszel test, stratifying according to age at killing (6 month and 1 year). The risk of tumors was significantly greater in *Muc2*^{-/-} than wild-type mice (odds ratio 8.956, *P* < 0.0001, Mantel-Haenszel test, StatXact, Cytel Software, Cambridge, MA). *n*, number of mice studied. Asterisk indicates mean ± SD.

Group (<i>n</i>)	No. mice with GI tumors			No. tumors per mouse		
	Total	Small intestine	Large intestine	Total	Small intestine	Large intestine
<i>Muc2</i> ^{+/+}						
6 months (6)	0	0	0	0	0	0
1 year (18)	0	0	0	0	0	0
<i>Muc2</i> ^{-/-}						
6 months (19)	3 (16%)	3 (16%)	0	0.32 ± 0.82*	0.32 ± 0.82	0
1 year (19)	13 (68%)	9 (47)	4 (21%)	1.58 ± 1.8	1.32 ± 1.8	0.26 ± 0.56

To assess the rate of migration of epithelial cells, we examined the fate of BrdU-labeled cells at 24 and 48 hours after BrdU injection. In the duodenum of wild-type mice, the majority of the cells had accumulated at the crypt-villous junction 24 hours after BrdU labeling (Fig. 1D). In contrast, in *Muc2*^{-/-} mice, a large number of BrdU⁺ cells had migrated into the proximal portion of the villous. Within 48 hours, all the BrdU⁺ cells had been shed from the villi of *Muc2*^{-/-} mice, whereas the majority of labeled cells were still present in the villi of wild-type mice (Fig. 1D). Similarly, at 24 hours the leading edge of BrdU⁺ cells was much higher up in the crypts of the distal colon of *Muc2*^{-/-} mice, and within 48 hours positive cells were detected at the top of the crypts. In contrast, BrdU⁺ cells had migrated only three-quarters of the crypt length of the wild-type mice (Fig. 1E). Thus, epithelial cells migrated faster in the intestinal mucosa of *Muc2*^{-/-} mice compared with wild-type mice.

Perturbation of the adenomatous polyposis coli (APC)-β-catenin pathway, as detected in familial adenomatous polyposis (FAP) patients and in the majority of sporadic colon cancers (12), results in nuclear accumulation of β-catenin and transcription of target genes including *c-myc* and *cyclin D1* (13, 14). Accordingly, tumors from *Apc1638* mice (15) showed strong nuclear expression of β-catenin and c-Myc (6), whereas tumors in *Muc2*^{-/-} mice displayed a strong c-Myc signal that was not accompanied by alterations in the levels and distribution of β-catenin (6). The alteration of c-Myc expression was specific for tumor cells because the pattern of c-Myc in the normal intestinal mucosa of wild-type and mutant mice was not markedly different (6). These results were confirmed by Western blot analysis (6).

In summary, our data demonstrate that *Muc2* functions in intestinal homeostasis and that its absence induces alterations that are manifested as increased proliferation, decreased apoptosis, and increased migration of intestinal epithelial cells. These alterations may be a secondary response to the absence of adequate

protection and lubrication and/or a primary response to changes in *Muc2* signaling. Inactivation of *Muc2* causes intestinal tumor formation with spontaneous progression to invasive carcinoma, and this occurs in the absence of the overt inflammatory response seen in other mouse models (16–18). The formation of rectal tumors also distinguishes the *Muc2*^{-/-} mouse from previous rodent models of intestinal tumorigenesis, and this mouse may represent a useful model to study human rectal cancers, which are clinically distinct entities of cancer (19). The reduced representation of goblet cells is characteristic of many aberrant crypt foci (ACF) of both humans and rodents (20, 21), which are considered early preneoplastic lesions (22–24). Our data support the hypothesis that the reduction in these cells and, thus, reduction of the mucus they produce, plays a role in tumor formation. Lastly, this work suggests that analysis of *MUC2* expression may provide

clinically useful information for prognosis and prevention of human colorectal cancer.

References and Notes

1. S. J. Gendler, A. P. Spicer, *Annu. Rev. Physiol.* **57**, 607 (1995).
2. Y. S. Kim, J. R. Gum, I. Brockhausen, *Glycoconj. J.* **13**, 693 (1996).
3. Y. S. Kim, J. R. Gum, *Gastroenterology* **109**, 999 (1995).
4. B. W. Van Klinken et al., *Am. J. Physiol.* **276**, G115 (1999).
5. F. Aslam, L. Palumbo, L. H. Augenlicht, A. Velcich, *Cancer Res.* **61**, 570 (2001).
6. Supplementary figures and details of experimental procedures are available on Science Online at www.sciencemag.org/cgi/content/full/295/5560/1726/DC1.
7. B. Sands, D. Podolsky, *Annu. Rev. Physiol.* **58**, 253 (1996).
8. L. Shekels et al., *Biochem. J.* **311**, 775 (1995).
9. L. L. Shekels et al., *Biochem. J.* **330**, 1301 (1998).
10. S. Williams et al., *J. Biol. Chem.* **276**, 18327 (2001).
11. A. Velcich et al., data not shown.
12. L. Su et al., *Science* **256**, 668 (1992).
13. T.-C. He et al., *Science* **281**, 1509 (1998).
14. O. Tetsu, F. McCormick, *Nature* **398**, 422 (1999).
15. R. Fodde et al., *Proc. Natl. Acad. Sci. U.S.A.* **91**, 8969 (1994).
16. U. Rudolph et al., *Nature Genet.* **10**, 143 (1995).
17. M. Hermiston, J. Gordon, *Science* **270**, 1203 (1995).
18. S. Engle et al., *Cancer Res.* **59**, 3379 (1999).
19. G. Steele et al., *J. Am. Med. Assoc.* **264**, 1444 (1990).
20. K. Otori, K. Sugiyama, T. Hasebe, S. Fukushima, H. Esumi, *Cancer Res.* **55**, 4743 (1995).
21. T. Pretlow, W. Edelman, L. Hudson Jr., R. Kucherlapati, L. Augenlicht, *Proc. Am. Assoc. Canc. Res.* **38**, 126 (1997).
22. R. Bird, *Cancer Lett.* **37**, 147 (1987).
23. T. B. Pretlow et al., *Cancer Res.* **51**, 1564 (1991).
24. I.-M. Siu et al., *Cancer Res.* **59**, 63 (1999).
25. Supported by NIH grants CA 72835, CA 90808, and PO CA 13330. We thank S. Einherand, S. Gendler, G. Hansson, S. Ho, C. Tomasetto, and D. Podolsky for providing reagents; G. Cattoretti for suggestions on c-Myc immunohistochemistry; L. Klampfer for stimulating discussions; and J. Mariadason for critically reading the manuscript.

17 October 2001; accepted 25 January 2002

Postsynaptic Induction of BDNF-Mediated Long-Term Potentiation

Yury Kovalchuk, Eric Hanse,* Karl W. Kafitz, Arthur Konnerth†

Brain-derived neurotrophic factor (BDNF) and other neurotrophins are critically involved in long-term potentiation (LTP). Previous reports point to a presynaptic site of neurotrophin action. By imaging dentate granule cells in mouse hippocampal slices, we identified BDNF-evoked Ca²⁺ transients in dendrites and spines, but not at presynaptic sites. Pairing a weak burst of synaptic stimulation with a brief dendritic BDNF application caused an immediate and robust induction of LTP. LTP induction required activation of postsynaptic Ca²⁺ channels and *N*-methyl-D-aspartate receptors and was prevented by the blockage of postsynaptic Ca²⁺ transients. Thus, our results suggest that BDNF-mediated LTP is induced postsynaptically. Our finding that dendritic spines are the exclusive synaptic sites for rapid BDNF-evoked Ca²⁺ signaling supports this conclusion.

Neurotrophins promote neuronal survival and differentiation, but it has become increasingly clear that they also have essential roles in synaptic plasticity (1–3). Exogenous BDNF

enhances transmission at the developing neuromuscular junction and at various central excitatory synapses (4–8). Furthermore, endogenous BDNF, via activation of the recep-